DOI: 10.1002/anie.201005105

Metal–Support Interfaces

Atomic Resolution of the Structure of a Metal–Support Interface: Triosmium Clusters on MgO(110)**

Apoorva Kulkarni, Miaofang Chi, Volkan Ortalan, Nigel D. Browning, and Bruce C. Gates**

Catalysts are the keys to control of chemical change, being essential for efficient production of chemicals, fuels, and polymeric materials and for pollution abatement. They are likely to be central to new technologies for biomass conversion. Many practical catalysts include metals, usually as nanoclusters or particles dispersed on a porous high-area metal oxide support. When the clusters consist of about 10 or fewer atoms, their properties differ from those of the bulk metal—and depend strongly on the cluster size and interactions with the support.[1] Metal–support interactions may be so significant that clusters of a particular metal on various supports can have widely different catalytic activities and selectivities, as illustrated, for example, by the performance of supported gold[2] and silver clusters.[3]

Determinations of nanocluster size and its importance on catalyst performance are now compelling, and high-resolution transmission electron microcopy (TEM) has played an important role in advancing the science.[4] Aberration-corrected scanning TEM (STEM) has recently been used to image individual metal atoms on[5] and in[6] supports, single layers of metal atoms on supports,[7] and clusters of only a few atoms each on[8] and in[6] supports. However, TEM imaging of supported metal nanoclusters has been restricted to the determination of cluster structures and sizes without characterization of the metal–support interface,[9] and understanding of support effects in catalysis remains limited.[10] There is a need for direct determination of atomic-scale structures of metal–support interfaces. Now we show how aberration-corrected STEM images of extremely small supported metal clusters, complemented by spectroscopy, provide structural information about the metal–support interface.

Our goal was to synthesize extremely small and uniform metal clusters on a support and characterize them with atomic-resolution STEM and extended X-ray absorption fine structure (EXAFS) spectroscopy to gain information about both the clusters and the support and the bonding between them. We used a compound of a Group 8 metal with metal–metal bonds as the precursor—$[Os_3(CO)_{12}]$, which has a stable triangular frame of Os atoms stabilized by the ligands. Our support was high-area powder MgO because it is commonly used in industrial catalysts and consists of highly crystalline particles that expose various faces. The quality of the sample was determined by the MgO calcination temperature (673 K), chosen because it is approximately the highest temperature suitable for decarbonation with partial dehydroxylation of this support without substantial reconstruction or thermal faceting.[11] The success of the synthesis of triosmium carbonyl clusters on MgO is borne out by the EXAFS spectra, indicating an average Os–Os coordination number of 2, within error, as in $[Os_3(CO)_{12}]$, with its triangular frame, and consistent within error with the adsorption of all the clusters with the metal frames intact. The EXAFS Os–Os distance (an average over the whole sample) is 2.89 Å, consistent with the removal of one CO ligand upon adsorption to form $[Os_3(CO)_{11}]^{2-}$, the expected surface species on the basic MgO.[12] Details are given in Supporting Information.

The combination of $[Os_3(CO)_{12}]$ and MgO is ideally suited to aberration-corrected Z-contrast STEM, because the heavy Os atoms are easily imaged on the light MgO support. Moreover, the triosmium clusters are small enough to allow imaging of each Os atom and to distinguish the atoms in the support—and thus to determine the exact sites where the clusters are anchored. Most MgO faces (e.g., Mg(100)) offer limited opportunities for the type of full structure determination shown here because it is impossible in a projected image to differentiate between Mg and O atoms on the surface (Mg and O are stacked alternately through the thickness of the sample (Mg-O-Mg···), with neighboring columns of atoms being out of phase with each other (O-Mg-O···). However, when the surface face is (110), then the underlying Mg and O atoms are separated into distinct atomic columns containing only one of these species (Mg-Mg-Mg··· or O-O-O···), and the faces can be readily distinguished by Z-

[*] A. Kulkarni, V. Ortalan, Prof. N. D. Browning, Prof. B. C. Gates
Department of Chemical Engineering and Materials Science
University of California
One Shields Avenue, Davis, CA 95616 (USA)
Fax: (+1) 530-752-1031
E-mail: nbrowning@ucdavis.edu
bcgates@ucdavis.edu
Homepage: http://www.chms.ucdavis.edu/research/web/catalysis
Prof. N. D. Browning
Chemistry, Materials and Life Sciences Directorate
Lawrence Livermore National Laboratory
700 East Avenue, Livermore, CA 94550 (USA)
Dr. M. Chi
Materials Science & Technology Division
Oak Ridge National Laboratory
Oak Ridge, TN 37830 (USA)

[**] This work was supported by the National Science Foundation, GOALI Grant CTS-05-00511, and by ExxonMobil. We acknowledge the National Synchrotron Light Source (NSLS), a national user facility operated by Brookhaven National Laboratory on behalf of the US Department of Energy (DOE), Office of Science, Basic Energy Sciences, for access to beam line X-18B. The electron microscopy experiments were performed at the Oak Ridge National Laboratory SHaRE User Facility, which is supported by the Division of Scientific User Facilities, DOE Office of Science, Basic Energy Sciences.

Supporting information for this article is available on the WWW under http://dx.doi.org/10.1002/anie.201005105.

contrast STEM imaging (Figure 1). Figure 2 shows images of the triosmium clusters on the (110) surface. It is clear that some clusters are fragmented (i.e., contain fewer than three atoms). Fragmentation of supported metal clusters can occur during synthesis or under the influence of the electron beam when the energy is high and/or the experiment prolonged.[13] To identify the clusters that were not affected by beam damage in each experiment, we restricted our consideration to those with a limited beam exposure and checked that the clusters were stable for several exposures.

The STEM images of the clusters on the MgO(110) face (Figure 2) identify the triosmium clusters (designated with circles in Figure 2) and also determine the locations of the surface Mg atoms as bright spots, thus distinguishing the individual rows of the MgO. The images determine the orientations of the clusters with respect to the Mg and O atoms of the (110) face. The striking results of Figure 2 are a) each Os atom is located atop an Mg atom and b) the Os atoms in each image of a triosmium cluster define a triangle that is well approximated as isosceles (but not equilateral), with the two equal Os–Os distances being less than the other one. The representative image of Figure 2 shows the presence of five intact triosmium clusters on MgO(110). Each has two Os atoms in one row and one in the immediate neighboring row. For example, the cluster labeled 1 in Figure 2 has one Os atom atop an Mg atom of row "a" and two Os atoms atop an Mg atom of the immediate neighbor row "b". On the other hand, one Os atom atop an Mg atom of row "b" and two Os atoms atop Mg atoms of neighbor row "a" characterize the clusters labeled 2, 3, 4, and 5.

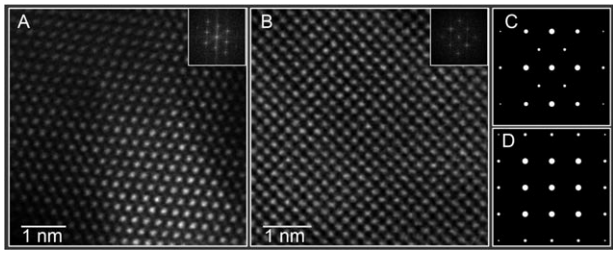

Figure 1. A,B) Aberration-corrected STEM images showing the presence of A) the bare MgO(110) surface with Mg and O atoms separated into distinct atomic columns containing only one of these species (Mg-Mg-Mg··· or O-O-O···), B) the bare MgO(100) surface with Mg and O atoms stacked alternately through the thickness of the sample (Mg-O-Mg···), with neighboring columns of atoms being O-Mg-O···. C,D) Simulated diffraction patterns of C) the MgO(110) surface and D) the MgO(100) surface. The insets in (A) and (B) represent the fast Fourier transforms (digital diffractograms).

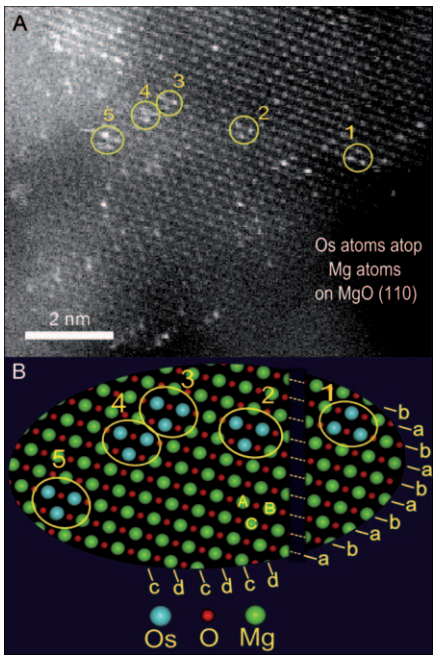

Figure 2. A) Aberration-corrected STEM image showing both individual Os atoms and Os atoms in triosmium clusters located atop Mg atoms in MgO(110); the encircled parts of the image show the intact supported triosmium clusters. The known structure of the MgO(110) surface provides a calibration of the metal–metal distances in the metal clusters on MgO, as shown in the lower part (B), which is a model of part of the STEM image showing the positions of the Os atoms.

Thus, by recognizing the Mg-O-Mg-O ridges on MgO-(110) surface, we see that there are two orientations of the triosmium clusters on MgO(110): a) one in which two of the Os atoms in a cluster are atop Mg atoms which are in a plane higher than that of the Mg atom on top of which the third Os atom is located (referred as orientation I) and b) one in which one of the Os atoms in a cluster is atop an Mg atom which is in a plane higher than that of the Mg atoms on top of which the other two Os atoms are located (orientation II). If the cluster labeled 1 is in orientation I, then the other encircled clusters are in orientation II and vice versa. We recognize that the triosmium frames shown in Figure 2 were not all in a plane perpendicular to the electron beam, because then they could not all be aligned directly above Mg atoms, as the images show them to be.

DFT calculations[14] show that metal clusters are bonded to MgO by metal–oxygen bonds,[15] consistent with the results observed generally by EXAFS spectroscopy for Group 8 metal clusters on metal oxides[16] and in agreement with our EXAFS results as well. (EXAFS data indicate distortion of CO ligands on adsorbed metal clusters to accommodate to the support surface.)[12b]

Any structural model of the triosmium clusters on MgO should account for the Os–O bonds. The images of the clusters shown in Figure 2 provide a basis for determining a model of the structures of the clusters that include the Os–oxygen bonds indicated by the EXAFS data[16] and DFT calculations.[15] We investigated all the models of the structures of the clusters on the MgO(110) face that match the data—that is, those having 3 Os atoms atop Mg atoms arranged in a triangle that is isosceles when viewed from the top and anchored through Os–O bonds. The models are based on the observed Os–Os distances and the structures of sites known to exist on MgO(110). In the model determination, the Os–$O_{support}$ distance (where $O_{support}$ is an oxygen atom on the MgO surface) was constrained between 2.1 and 2.2 Å, consistent with EXAFS data for our sample and Group 8 metal clusters on supports generally.[16] The results are summarized in Figure 3. The models account for the possible interactions of Os atoms in trinuclear clusters with oxygen atoms of the support.

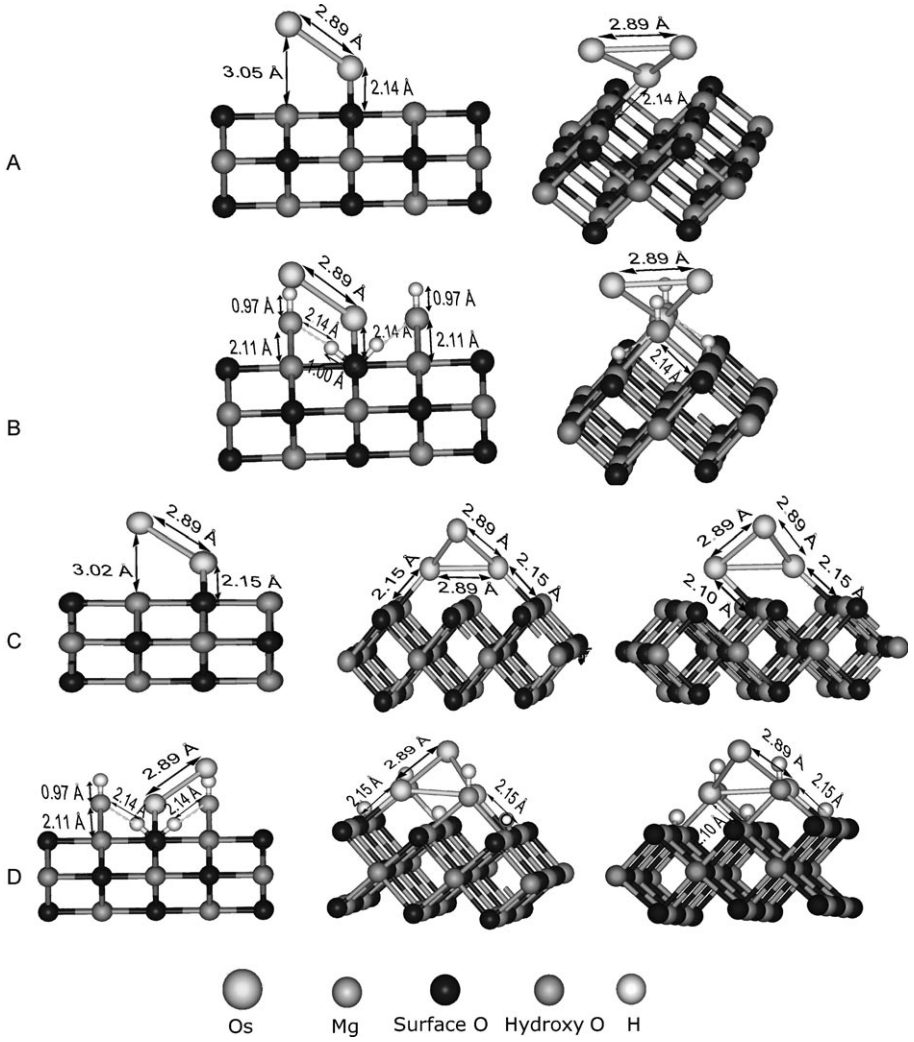

Figure 3. Structural models of supported triosmium clusters on MgO(110) depicting the Os–support interactions on hydroxylated MgO(110) and on dehydroxylated MgO(110); side views and perspective views are shown. A) Triosmium cluster orientation I on dehydroxylated MgO(110); B) triosmium cluster orientation I on hydroxylated MgO(110); C) triosmium cluster orientation II, including two models for dehydroxylated MgO(110); and D) triosmium cluster orientation II, including two models for hydroxylated MgO(110). The hydroxylated surfaces consist of hydroxy groups on surface Mg atoms and protons on neighboring surface O atoms. The structure and bonding distances of adsorbed hydroxy groups and hydrogen bonding between hydroxy O atoms and protons on surface O atoms were estimated on the basis of reported DFT calculations.[11b,c]

The structures of the models represented in Figure 3 match the observation of the Os atoms atop Mg atoms (as shown in Figure 3). The models were determined both for hydroxylated and dehydroxylated MgO(110) surfaces and for both orientations I and II of the triosmium clusters. Each model (three each for hydroxylated MgO(110) and dehydroxylated MgO(110)) shown in Figure 3 is consistent with the data; in each, Os is bonded to a surface O atom of MgO.

The triosmium frame in each model is tilted with respect to the MgO(110) surface, and the tilt angle depends on the geometry and the Os–$O_{support}$ distance. The triosmium frames both in orientation I and orientation II are tilted at an angle of 38° with respect to the MgO(110) surface; this is evidently the condition for bonding of the triosmium clusters atop Mg atoms so that the Os–$O_{support}$ and Os–Os distances are in agreement with the EXAFS results.

On the basis of this tilt angle we calculated the Os–Os distances in the clusters determined by the STEM images represented in Figure 2 (the images represent projections of the Os–Os distances at 38°). The triosmium frames in each orientation (I and II) viewed from the top appear as isosceles triangles with the length of the longer side being (3.02 ± 0.21) Å and that of the shorter side being (2.20 ± 0.21) Å. By correcting the lengths of the sides for the projection at 38°, we calculated the Os–Os distance of the shorter sides to be 2.80 Å. Thus the average of two distances of 2.80 Å and one distance of 3.02 Å is 2.87 Å, which within error matches the average Os–Os distance of (2.89 ± 0.06) Å determined by EXAFS spectroscopy for the sample as a whole (i.e., that with osmium clusters on all the MgO faces). This comparison suggests similar average Os–Os distances in the triosmium clusters on the various MgO faces. We lack the data to determine the Os–O coordination numbers of the clusters on the various faces (the average Os–O coordination number determined by the EXAFS data is 1.0), although it is clear that adsorption of the clusters on MgO results in distortion and/or reorientation of the CO ligands to accommodate the metal–support interaction, as shown by the broadening of the IR bands in the ν_{CO} region, as expected.[12b] On the dehydroxylated MgO(110) surface, the clusters can bond to the surface O atoms, whereby each Os atom may be bonded to one O atom or none. This non-uniform bonding between Os and surface O atoms of MgO probably occurs because the Mg(110) surface has Mg-O-Mg-O ridges which inherently present dissimilar bonding sites for the Os atoms.

Our treatment of the MgO removed most of the surface OH groups;[17] these arise in the original sample from chemisorption of water on MgO, which occurs dissociatively, resulting in hydroxylation of Mg^{2+} sites and protonation of O^{2-}.[14] There is agreement that on a perfect MgO(100) surface, which consists of five-fold coordinated sites, the chemisorption of water is energetically unfavorable and instead takes place at three- or four-fold coordinated sites such as kinks, corners, or edges. On the other hand, the Mg-O-

Mg-O ridges along the (001) direction of MgO(110) expose both Mg and O atoms that are four-fold coordinated. Calcination leads to removal of water and of surface OH groups from MgO.[17]

DFT calculations by Rösch and co-workers[14] have shown that the strength of the metal–$O_{support}$ bonds (where $O_{support}$ is oxygen of the MgO surface and the metal is Re) can be markedly reduced by hydroxylation of the MgO surface. Thus, this dehydroxylation makes four-fold coordinated sites on MgO(110) available for bonding with osmium clusters. Calculations[14] have shown that the bonding of a Re atom to MgO is facilitated by the introduction of point defects on MgO(100) where Mg is four-fold coordinated. Because the Mg atoms on MgO(110) are four-fold coordinated, we suggest that they may be similar in reactivity to the defect sites on MgO(100).[11b] Therefore, we might expect the (110) surface to be more reactive with $[Os_3(CO)_{12}]$ than MgO(100).[11b]

A major difference between the bonding of metal atoms to hydroxylated and to dehydroxylated MgO surfaces is the strength of bonding;[14] metals are generally more weakly bonded to the hydroxylated surfaces, which accounts for their relatively high susceptibility to sintering on such surfaces.

In summary, the results presented here provide direct evidence of the structure of a metal–support interface. Understanding of metal–support interactions will help in the design of supported metal nanocluster catalysts and the prediction of their properties. We anticipate that these results will help elucidate how metal clusters interact with metal oxides and zeolites generally.

Experimental Section

MgO powder (EM Science, surface area 70 $m^2 g^{-1}$) was calcined in O_2 at 673 K for 6 h and evacuated at 673 K for 14 h, isolated, and stored in an argon-filled glovebox with < 1 ppm O_2 and < 1 ppm water. The precursor $[Os_3(CO)_{12}]$ reacted with the treated MgO in a slurry in dried, deoxygenated *n*-pentane at 273 K. The Os content of the resultant powder was 1.0 wt%. Details are reported in the Supporting Information.

EXAFS experiments were performed at X-ray beam line X-18B at the National Synchrotron Light Source at Brookhaven National Laboratory. The storage ring operated with an electron energy of 3 GeV. The ring current was in the range 60–100 mA. In an argon-filled glovebox at the synchrotron, each powder sample was pressed into a self-supporting wafer. The sample mass was chosen to give an X-ray absorbance of 2.5 at the Os L_{III} edge (10871 eV). The wafer was loaded into a cell (S4), sealed under a positive N_2 pressure, and removed from the glovebox. The cell was then evacuated (10^{-5} mbar), and the sample was aligned in the X-ray beam and cooled to nearly liquid-nitrogen temperature. EXAFS spectra were then collected in transmission mode. Higher harmonics in the X-ray beam were minimized by detuning the Si(111) monochromator by 20–25% at the Os L_{III} edge. The reported spectrum is the average of four individual scans.

The samples in stainless-steel tubes (sealed with O-rings) that are commonly used for handling samples for ultrahigh-vacuum experiments were transported to Oak Ridge National Laboratory (ORNL) for microscopy experiments. At ORNL, the samples were handled in an argon-filled glove bag, which was purged 20 times with argon before use. The tubes containing the sample were opened in the glove bag, and the samples were placed onto copper grids (200 mesh). The sample holder was transferred from the glove bag to the microscope with an air exposure of at most approximately 2 s. High-resolution STEM-HAADF images of the sample were acquired with an aberration-corrected JEOL 2200 FS microscope, with the convergence angle being 26.5 mrad and the collection inner angle 100 mrad. To minimize the artifacts in the images caused by beam damage, the microscope was aligned for one region of the sample, and then the beam was shifted to a neighboring region for a quick image acquisition: 4 s for a 512×512 pixel size. This methodology ensured that the exposure of the imaged area to the electron beam was minimal.

Details of experimentation and data analysis are given in the Supporting Information.

Received: August 16, 2010
Published online: November 25, 2010

Keywords: aberration-corrected STEM · metal–support interfaces · MgO · molecular clusters · surface chemistry

[1] a) A. M. Argo, J. F. Odzak, F. S. Lai, B. C. Gates, *Nature* **2002**, *415*, 623; b) Z. Xu, F. S. Xiao, S. K. Purnell, O. Alexeev, S. Kawi, S. E. Deutsch, B. C. Gates, *Nature* **1994**, *372*, 346.
[2] A. Grirrane, A. Corma, H. Garcia, *Science* **2008**, *322*, 1661.
[3] Y. Lei, F. Mehmood, S. Lee, J. Greeley, B. Lee, S. Seifert, R. E. Winans, J. W. Elam, R. J. Meyer, P. C. Redfern, D. Teschner, R. Schlögl, M. J. Pellin, L. A. Curtiss, S. Vajda, *Science* **2010**, *328*, 224.
[4] a) P. D. Nellist, S. J. Pennycook, *Science* **1996**, *274*, 413; b) K. Sohlberg, S. Rashkeev, A. Y. Borisevich, S. J. Pennycook, S. T. Pantelides, *ChemPhysChem* **2004**, *5*, 1893; c) A. K. Datye, *J. Catal.* **2003**, *216*, 144.
[5] A. Uzun, N. D. Browning, B. C. Gates, *Chem. Commun.* **2009**, 4657.
[6] V. Ortalan, A. Uzun, B. C. Gates, N. D. Browning, *Nat. Nanotechnol.* **2010**, *5*, 506.
[7] C. Kisielowski, Q. Ramasse, L. Hansen, M. Brorson, A. Carlsson, A. Molenbroek, H. Topsøe, S. Helveg, *Angew. Chem.* **2010**, *122*, 2768; *Angew. Chem. Int. Ed.* **2010**, *49*, 2708.
[8] A. Uzun, V. Ortalan, Y. Hao, N. D. Browning, B. C. Gates, *ACS Nano* **2009**, *3*, 3691.
[9] G. J. Hutchings, M. S. Hall, A. F. Carley, P. Landon, B. E. Solsona, C. J. Kiely, A. Herzing, M. Makkee, J. A. Moulijn, A. Overweg, J. C. Fierro-Gonzalez, J. Guzman, B. C. Gates, *J. Catal.* **2006**, *242*, 71.
[10] a) C. M. Y. Yeung, K. M. K. Yu, Q. J. Fu, D. Thompsett, M. I. Petch, S. C. Tsang, *J. Am. Chem. Soc.* **2005**, *127*, 18010; b) J. H. Kwak, J. Hu, D. Mei, C.-W. Yi, D. H. Kim, C. H. F. Peden, L. F. Allard, J. Szanyi, *Science* **2009**, *325*, 1670.
[11] a) V. E. Henrich, *Surf. Sci.* **1976**, *57*, 385; b) D. Costa, C. Chizallet, B. Ealet, J. Goniakowski, F. Finocchi, *J. Chem. Phys.* **2006**, *125*, 054702; c) N. H. de Leeuw, G. W. Watson, S. C. Parker, *J. Phys. Chem.* **1995**, *99*, 17219.
[12] a) R. Psaro, C. Dossi, R. Ugo, *J. Mol. Catal.* **1983**, *21*, 331; b) V. A. Bhirud, H. Iddir, N. D. Browning, B. C. Gates, *J. Phys. Chem. B* **2005**, *109*, 12738.
[13] P. E. Batson, N. Dellby, O. L. Krivanek, *Nature* **2002**, *418*, 617.
[14] A. Hu, K. M. Neyman, M. Staufer, T. Belling, B. C. Gates, N. Rösch, *J. Am. Chem. Soc.* **1999**, *121*, 4522.
[15] J. F. Goellner, K. M. Neyman, M. Mayer, F. Noertemann, B. C. Gates, N. Rösch, *Langmuir* **2000**, *16*, 2736.
[16] J. C. Fierro-Gonzalez, S. Kuba, Y. Hao, B. C. Gates, *J. Phys. Chem. B* **2006**, *110*, 13326.
[17] H. Dunski, W. K. Józwiak, H. Sugier, *J. Catal.* **1994**, *146*, 166.
[18] R. E. Jentoft, S. E. Deutsch, B. C. Gates, *Rev. Sci. Instrum.* **1996**, *67*, 2111.
[19] D. C. Koningsberger, B. L. Mojet, G. E. van Dorssen, D. E. Ramaker, *Top. Catal.* **2000**, *10*, 143.

